

Article

Quantifying Raptors' Flight Behavior to Assess Collision Risk and Avoidance Behavior to Wind Turbines

Anne Cathrine Linder ^{1*} , Henriette Lyhne ¹, Bjarke Laubek ², Dan Bruhn ^{1,3}  and Cino Pertoldi ^{1,4} 

¹ Department of Chemistry and Bioscience — Section of Biology and Environmental Science, Aalborg University, Fredrik Bajers Vej 7, 9220 Aalborg, Denmark; c.linder04@gmail.com (A.C.L.); henry.lyhne@hotmail.com (H.L.); db@bio.aau.dk (D.B.); cp@bio.aau.dk (C.P.)

² Vattenfall Renewable Wind DK A/S, Jupitervej 6–2nd floor, 6000 Kolding, Denmark; bjarke.laubek@vattenfall.com (B.L.)

³ Skagen Bird Observatory, Fyrvej 36, 9990 Skagen, Denmark

⁴ Aalborg Zoo, Mølleparkvej 63, 9000 Aalborg, Denmark

* Correspondence: c.linder04@gmail.com

1 Simple Summary: An increasing amount of wind turbines installed worldwide has in turn lead
 2 to an increase in bird fatality due to collisions. This conservation threat has led to the development
 3 of automated camera-based monitoring systems, that have recently been installed on some wind
 4 energy sites to mitigate the impact of wind turbines on protected raptors. This study describes a
 5 new quantitative framework to assess birds' flight behavior in proximity to wind turbines based
 6 on data from these camera-based monitoring systems. It is demonstrated how this novel method
 7 for describing flight behavior can be used to identify risk prone behavior, which is a crucial step
 8 towards quantifying collision risk with wind turbines.

9 Abstract: Some wind farms have implemented automated camera-based monitoring systems e.g.
 10 IdentiFlight to mitigate the impact of wind turbines on protected raptors. These systems have
 11 effectuated the collection of large amounts of data that can be used to describe flight behavior in
 12 a novel way. This data uniquely provides both flight trajectories and images of individual birds
 13 throughout their flight trajectories. The aim of this study was to evaluate how this unique data
 14 could be used to create a robust quantitative behavioral analysis, that could be used to identify
 15 risk prone flight behavior and avoidance behavior thereby in the future assess collision risk. This
 16 was attained through a case study at a wind farm on the Swedish island Gotland, where golden
 17 eagles (*Aquila chrysaetos*), white-tailed eagles (*Haliaeetus albicilla*), and red kites (*Milvus milvus*),
 18 were chosen as the selected bird species. The results demonstrate that flight trajectories and bird
 19 images can be used to identify high risk flight behavior and thereby also used to evaluate collision
 20 risk and avoidance behavior. This study presents a promising framework for future research,
 21 demonstrating how data from camera-based monitoring systems can be utilized to quantitatively
 22 describe risk prone behavior and thereby assess collision risk and avoidance behavior.

23 Keywords: IdentiFlight, avoidance response, golden eagle, white-tailed eagle, red kite, wind
 24 turbine curtailment, flight types

25 1. Introduction

26 Wind energy production has over the past decades undergone a rapid development,
 27 due to the increasing demand for green energy. However, the increasing amount of
 28 wind turbines installed worldwide has in turn lead to an increase in bird fatality, due
 29 to collisions, particularly regarding raptors [1–7]. Loss *et al.* [7] estimated that bird
 30 fatality increases proportionally with increasing turbine height. The exact number of
 31 bird collisions with turbines is uncertain, but even relatively low mortalities can have a
 32 significant impact on slow maturing species with low reproduction rates e.g. raptors,
 33 especially when considering the cumulative effect of multiple wind farms [1,7].

Collision risk is assumed to be dependent on flight behavior, where some types of behavior e.g. flying at altitudes within turbine rotor zone and tortuous flight paths, have been described as more risk prone than others [6]. Another suggested predictor of collision risk is whether birds are migrating or engaging in local activities e.g. foraging, as foraging individuals are expected to be less vigilant in regard to their flight direction and more focused on searching for prey on the ground [1,6,8,9]. Moreover, flight type is another behavioral factor suggested to affect collision risk. Large raptors such as golden eagles (*Aquila chrysaetos*), depend upon soaring flight to retain energy, this flight type may however increase their risk of colliding with turbines, especially under less favorable conditions for gaining altitude [10–13]. Barrios and Rodríguez [10] found an increased collision rate when birds were forced to gain altitude using thermal soaring, i.e. slow circle-soaring flight on thermals, which often took place in airspace overlapping with turbines. Hence, flight type and thereby also collision risk are suggested to be affected by environmental factors such as weather (e.g. wind speed and direction, temperature, cloud coverage, and visibility) and topography [10,14]. Furthermore, the risk of collision is presumably also strongly affected by avoidance behavior [9].

Avoidance behavior is generally observed as changes in flight behavior and trajectories in response to wind turbines, this avoidance response can be found at different scales i.e. micro-scale (last second) and meso-scale (within wind farm) avoidance responses to single turbines within a wind farm and macro-scale avoidance responses, avoiding the entire wind farm [13,15]. Garvin *et al.* [9] defined avoidance as changes in flight height or flight direction deviating away from turbines and found that raptors showing no response to turbines were individuals passing through the wind farm on a straight flight path. It has been suggested that raptors are more vulnerable to turbines due to lower avoidance compared to the avoidance of migratory species e.g. geese [16]. Dahl *et al.* [14] showed that white-tailed eagles displayed high risk flight behavior i.e. no flight response and lack of avoidance close to turbines, which was also associated with high collision rates. However, multiple other studies have also found implications of raptors adjusting their flight trajectories to avoid wind turbines [17,18]. Whitfield and Madders [17] showed that red kites displayed avoidance rates between 98 and 100%. These contradicting findings indicate that avoidance behavior is both site- and species-specific [3,9,19]. It is therefore necessary to gain an understanding of which variables affect flight behavior in general for specific species and sites to gain a more thorough understanding of avoidance behavior.

Regardless of avoidance behavior, some protected raptor species have been suggested to be more vulnerable to wind turbines and the impact of wind turbines on such species may, therefore, be mitigated by turbine curtailment [20]. Some wind farms, particularly in the United States, have implemented an automated camera-based monitoring system e.g. IdentiFlight, to detect birds in flight and determine whether they are protected species e.g. eagles. If a bird, that is detected as one of the protected species, has a calculated trajectory on course to a turbine or is within a specified radius of a wind turbine, the wind turbine will curtail before a collision occurs [21]. However, the actual collision risk between raptors and wind turbines is presumably determined by the vigilance of individuals i.e. their avoidance behavior, which is suggested to be dependent on multiple factors, e.g. weather conditions [9,14,15,22]. Knowledge on the avoidance behavior of protected raptors, such as eagles and the red kite, and how this behavior can be affected by environmental factors is therefore crucial to improving curtailment decisions. Curtailing wind turbines is expensive and energy companies would, therefore, benefit from the development of behavior specific curtailment models. Furthermore, the IdentiFlight camera system can provide a useful service to avian biologists, as it enables the collection of large amounts of data with a large number of individuals, compared to studies using GPS trackers, requiring the capture of birds and thus limiting the number of individuals. A system such as IdentiFlight provides not only flight trajectories based on GPS coordinates, but also images of individual birds throughout their flight trajec-

ries, thus giving the unique opportunity of assessing flight behavior based on both flight trajectories and behavioral observations i.e. flight orientation.

The development of camera-based monitoring systems at wind farms has effectuated the collection of large amounts of data that can be used to describe the behavior of selected bird species, thus, enabling the possibility of creating robust quantitative behavioral analyses, which may be used to assess collision risk and avoidance behavior, potentially providing avian biologists with new imperative knowledge. Therefore, this study will investigate how the behavior of raptors can be quantified by using unique data from the IdentiFlight system, demonstrating how this type of data can be used to assess collision risk and investigate site and species-specific avoidance behavior. This was achieved through a case study investigating the behavior of golden eagles (*Aquila chrysaetos*), white-tailed eagles (*Haliaeetus albicilla*), and red kites (*Milvus milvus*) at a wind farm on the Swedish island Gotland. It was a prerequisite that the flight behavior of these species could be described by flight altitude, flight trajectories, active flight, and flight orientation i.e. head position. It was expected that these variables could be used to describe risk prone behavior e.g. tortuous flight and thereby utilized as an indicator of collision risk. Flight behavior was also predicted to be affected by weather variables, e.g. temperature, wind speed and cloud coverage and may therefore be factor to be considered when predicting collision risk. It was furthermore expected that avoidance behavior could be detected through the new quantitative assessment of flight behavior in proximity to wind turbines.

2. Materials and Methods

2.1. Study Site

The study site is situated on Näsudden, a peninsula on Gotland’s southwest coast. The terrain is generally flat and the highest peak of the island is only 135 meters above sea level [23]. Gotland is home to breeding populations of approximately 55 pairs of the golden eagle, 45 pairs of the white-tailed eagle and at least 15 pairs of the red kite [24,25]. The island is not directly part of any migratory routes for these species and these species are therefore mainly represented by local individuals [26]. The wind farm consists of 55 turbines, ranging from 45–145 meters in total height. The first turbines were constructed in 1979. The observational area of the wind farm was defined by a radius of 400 meters around the IdentiFlight camera tower and included nine turbines (Appendix A).

2.2. Data Collection

Observations of the selected species were collected using the IdentiFlight system over a period of 10 months in 2020, spanning from the middle of February to the end of November. During the study period the IdentiFlight system was only collecting simulated curtailment data for the nine turbines, hence, the system was not actively curtailing turbines. Throughout this period of time, the system was periodically out of operation and the study is therefore based on a total of 231 days over the course of these 10 months (Appendix B). Out of the 231 days, raptors of the species golden eagle, white-tailed eagle or red kite were only observed within the observational area of the wind farm on 153 of these days.

2.2.1. IdentiFlight System

The IdentiFlight system was developed to detect eagles at risk of collision with a rotating wind turbine. The system can detect a bird as far as one kilometer out and classify whether it is a protected species or not in real time and determine if a specific turbine or turbines should be shut down to prevent collision, based on a set of site-specific criteria (curtailment prescription) [21,27]. The curtailment prescription for the study site can be found in Appendix C.1.

The camera system consists of a ring of eight fixed Wide Field of View (WFOV) cameras and a set of High Resolution Stereo Cameras (HRSC) mounted on top of a six

meter high tower (Appendix C.2). The eight WFOV cameras use image sensor arrays to detect moving objects in the environment and begin to track them. These cameras collect 10 frames per second and detect objects moving from one frame to the next. When a moving object is detected two movable HRSCs are directed at the object. The HRSC uses high magnification stereoscopic sensors to determine the distance to the object and gathers the necessary information to classify the object. IdentiFlight's machine vision algorithms use a catalog of rules that have been developed by pattern recognition technology to analyze the images obtained by the HRSC. Size, plumage, color, wing shapes and flight profiles are some of the variables used to classify a bird [27].

The IdentiFlight system provides a data set with a large variety of variables, including bird images, describing each observation and giving each individual a unique Track ID (Appendix D). Furthermore, flight trajectories for each individual are saved as Keyhole Markup Language (KML: a file format used to display geographic data) files, which can be imported into ArcGIS Pro [28]. Thus, resulting in a data set with multiple observations of each individual and a single track based on these observations i.e. the flight trajectory of an individual's flight path illustrating its observed flight activity. Hereafter, when referring to observations it is a reference to all observations (multiple observation for each individual) and when referring to tracks it is a reference to the individuals' flight trajectories i.e. all observations summarized for each individual (each track represents one individual).

2.2.2. Weather Data

Temperature, wind speed and wind direction, provided by Vattenfall AB [29], was collected at 10 minute intervals by weather stations on the turbines at a height of 80 meters, hence portraying the weather conditions near the rotor zone of the turbines. Cloud coverage at hourly intervals was downloaded from the Swedish Meteorological and Hydrological Institute [30].

2.3. Data Preparation

Observations from the data collected were filtered based on the species classified by the system in order to obtain a subset with the species golden eagle, white-tailed eagle, and red kite. The bird images were used to classify the head position of the raptors, as either oriented straight forward or down and whether or not the raptor was engaging in

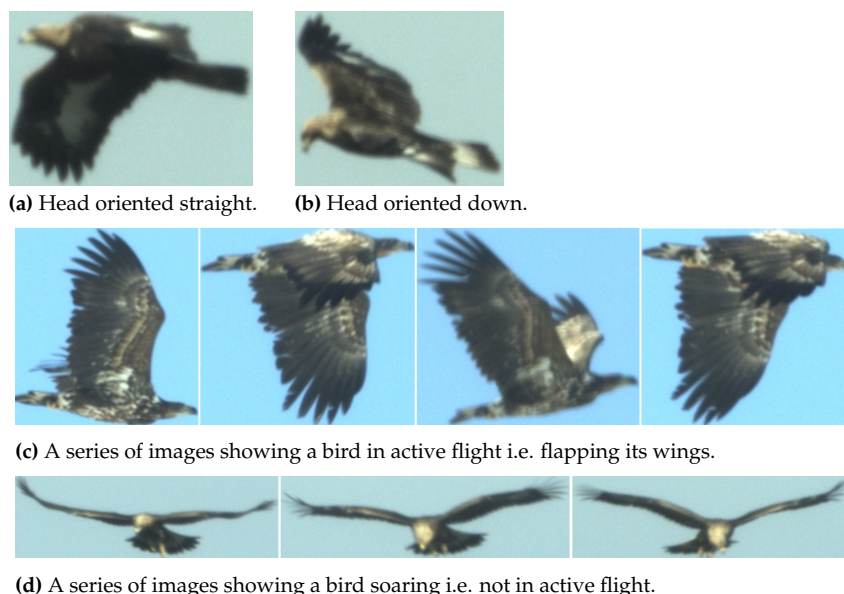


Figure 1. Examples of how behavior was scored based on bird images, a single image was used to classify head position and a series of images had to be used to classify active flight in order to evaluate wing movement between images.

active flight (Figure 1). Only observations within 400 meters of the camera system were used, as it was difficult to classify the head position for images taken at further distances (Appendix A). Furthermore, only tracks longer than 100 meters were used, as shorter tracks were not considered to be fully descriptive of an individual’s behavior within the area. This resulted in a data set of 564 different tracks (individuals) of the three selected species (Appendix E).

ArcGIS Pro [28] was used to analyze the flight trajectories (KML files). The flight trajectories were used to classify flight type i.e. each individual was assigned one of four different flight types based on a qualitative assessment of flight trajectories. The four different flight types used to describe the flight paths were straight, curvy, spiral, and chaotic (Figure 2). The flight type straight describes raptors flying in a linear path with only minor directional deviations. Raptors flying in the same general direction, but with slightly larger directional deviations than those depicted as straight were classified as the flight type curvy. The flight type spiral represents raptors presumed to be using thermal soaring i.e. soaring in updrafts using thermal convection, thus directional changes were mainly in the same direction, creating loops while increasing altitude. When a raptor’s flight path had no general flight direction and many large directional changes in both directions, the flight type was categorized as chaotic.

The flight trajectories were also assessed by calculating the track angles and the ratio between direct track length, i.e. the shortest distance between a track’s start point and its end point, and actual track length, which was done using the ArcPy package in Esri [28] (Appendix F.1 & F.2). The track angles ranged from -180° to 180° , distinguishing between left and right turns. Moreover, directional changes i.e. signed track angles were summed for each track, resulting in a measure of flight symmetry (Appendix F.2). The absolute sum of track angles and track length ratio were used to assess the qualitative classification of track types.

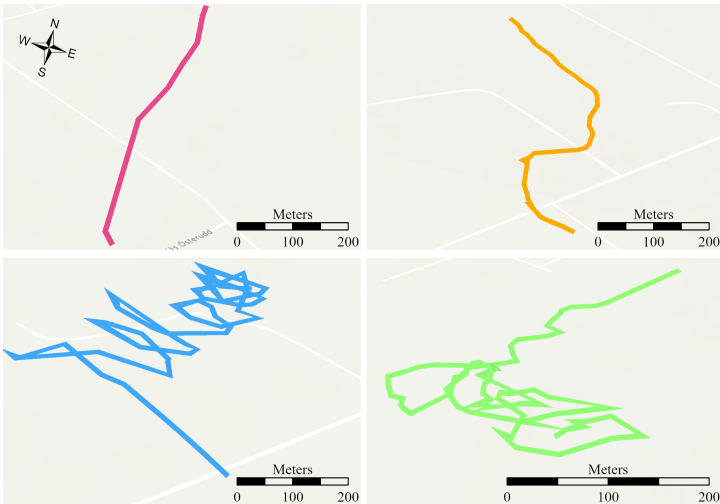


Figure 2. Examples of the four different track types: straight (pink), curvy (orange), spiral (blue), and chaotic (green). The images are based on three-dimensional tracks, i.e. multiple points with x, y and z coordinates.

2.4. Data Analysis

The data analyses were carried out for all observations, but also for subsets of observations based on track type, flight type, flight direction, flight altitude and distance to turbine (Appendix E). For analyses involving head orientation or active flight only individuals with more than three observations (bird images) were used. All tracks were divided into four subsets based on track type. Another subset was created only including tracks with individuals engaging in active flight. All observations were divided into two subsets based on flight direction i.e. flying towards the wind turbine

or away from the wind turbine, this was based on whether the distance to the nearest turbine was decreasing or increasing, meaning that most individuals are present in both subsets, as throughout their track they both fly towards and away from a turbine. Furthermore, three subsets were created dividing observations based on flight altitude into the categories: below, in or above the rotor zone of the nearest turbine i.e. each individual could be represented in multiple subsets (see Appendix C.1 for rotor zone definitions). Lastly, two subsets were created dividing all observations based on the distance to the nearest turbine into the categories: close proximity to turbine (<150 m) and distant to turbine (>150 m) i.e. each individual could be represented in multiple subsets. This distance of 150 meters was based on initial observations indicating changes in behavior at this distance. The statistical analyses were conducted in RStudio version 1.3.1093 [31].

2.4.1. Flight Behavior Classifications

To assess how the general flight behavior of raptors can be quantified and how it is affected by the weather, associations both among the different variables describing flight behavior and between these variables and weather variables were tested with the χ^2 contingency test and Spearman's rank correlation (r_s) [32]. Significant results are annotated * when $p < 0.05$; ** when $p < 0.01$; and *** when $p < 0.001$. Bonferroni's correction for multiple comparisons was not applied as the data were interdependent [32]. For the χ^2 contingency test, continuous variables such as % time spent looking down, % time spent on active flight, distance to nearest turbine, and weather variables were described as categorical variables e.g. temperature was categorized as low (0–10 °C), medium (10–20 °C) or high (20–30 °C) temperatures.

In order to evaluate the applicability of sum of directional changes and track length ratio, as indicators of the overall track type, a box plot of each variable was created, describing median and interquartile range (25%–75%) for each track type. Furthermore, associations between track type and flight behavior and weather variables, described as categorical variables, were assessed using the χ^2 contingency test along with bar plots depicting the proportions. To test the correlation between different variables describing flight behavior (i.e. head position as % time spent looking down, flight altitude, sum of directional changes and track length ratio) and various weather variables (i.e. temperature, wind speed and cloud coverage), correlation coefficients were calculated and the relationships between these variables were visualized with linear regressions. All regressions were based on grouped medians of the dependent variable, that were determined by class intervals of independent variables, with horizontal bars representing the interquartile range (IQR) to illustrate the variation around the medians. This was done for all subsets.

2.4.2. Avoidance Behavior

To assess avoidance behavior, i.e. behavioral changes, such as changes in flight altitude, in proximity to wind turbines, r_s was calculated for distance to nearest turbine in relation to the variables describing flight behavior i.e. flight orientation (% time spent looking down) and flight altitude, and the relationships between these variables were also visualized with linear regressions based on grouped medians. This was also done for all subsets. It was assumed that avoidance behavior would only be observed within a certain radius of a wind turbine. Therefore, the cumulative regression between distance to nearest turbine and flight altitude was calculated with increasing turbine distance, to find the distance at which the relationship weakened. This distance was hereafter used as an upper limit for the analysis of avoidance behavior. This was done for all subsets used in this analysis and the upper limit varied across subsets.

253 **3. Results**
254 *3.1. Flight Behavior Classification*

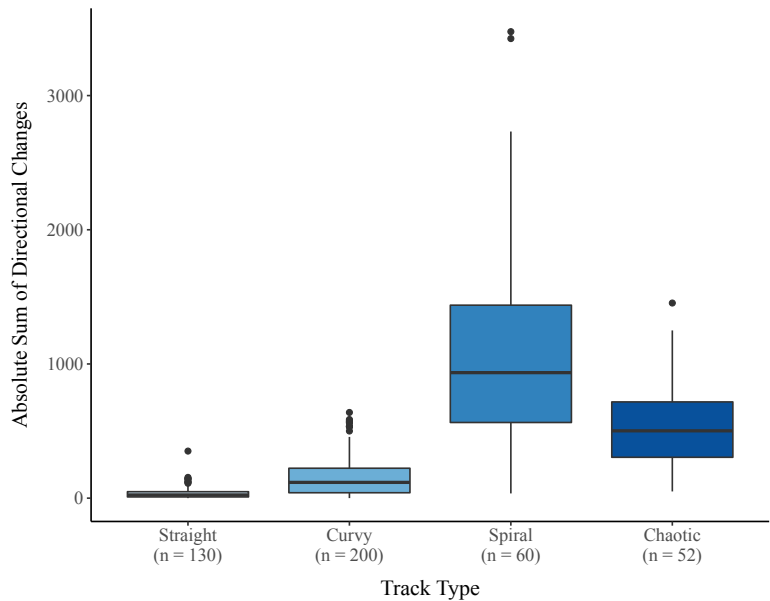


Figure 3. The absolute sum of directional changes grouped by track type. The number of tracks each subset is based on is annotated under each track type.

255 A difference was found in sum of directional changes between the different track
256 types, where straight and curvy flight types had a lower absolute sum of directional
257 changes and spiral flight types had the highest sum of directional changes (Figure 3).
258 Moreover, there was also a clear difference between the track length ratio of different
259 track types, where straight tracks had the largest track length ratios (IQR = 0.935–0.982).
260 Curvy tracks also had large track length ratios (IQR = 0.510–0.827), in comparison to
261 spiral (IQR = 0.216–0.467) and chaotic tracks (IQR = 0.171–0.477), between which there
262 was no observable difference (Figure 4).

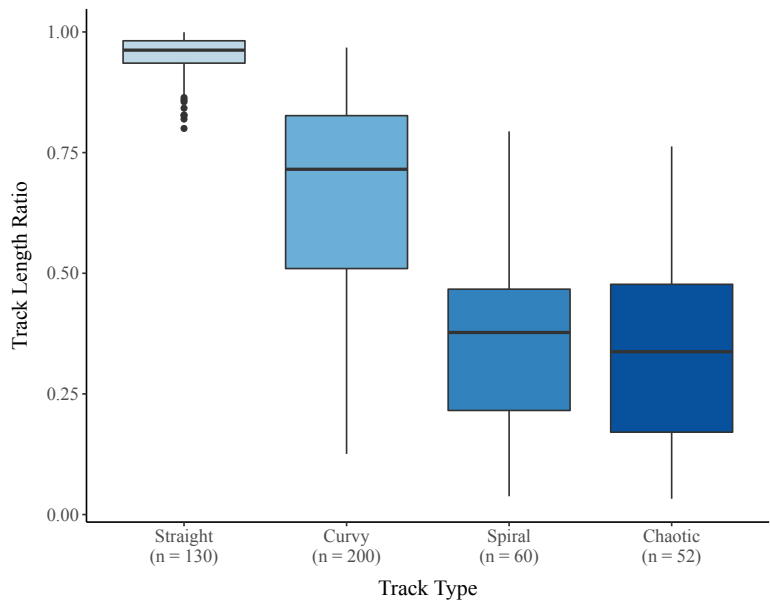


Figure 4. The ratio between the shortest path from a track's start to end point and the actual track length, grouped by track type. The number of tracks each subset is based on is annotated under each track type.

263 An association was found between time spent looking down and flight type ($\chi^2_9 =$
 264 55.8***) (see Appendix G for all χ^2 values). When flying in a straight or curvy flight
 265 pattern raptors spent less time looking down and when flying in a chaotic or spiraling
 266 pattern they spent more time looking down (Figure 5a). There was also found an
 267 association between time spent on active flight and flight type ($\chi^2_9 = 65.3^{***}$). More
 268 particularly, it was found that individuals flying in chaotic or spiraling patterns generally
 269 spent a small proportion of time (< 33%) on active flight (Figure 5b). Furthermore, flight
 270 type was found to be dependent on the height zone at which flight activity took place
 271 ($\chi^2_6 = 38.2^{***}$). Most of the individuals flying below the rotor zone were flying in
 272 straight (40.1%) or curvy (50.3%) patterns (Figure 5c). For individuals flying above the
 273 rotor zone there was a larger variation between the flight patterns utilized. A large
 274 proportion of the individuals flying in curvy (45.5%) or chaotic (55.8%) patterns were
 275 flying in the rotor zone. Flight type was also associated with distance to the nearest
 276 turbine ($\chi^2_9 = 18.6^*$), where it was found that most of the individuals flying near
 277 turbines were flying in straight or curvy patterns. The proportion of individuals flying
 278 in curvy or chaotic patterns increased with distance to the nearest turbine (Figure 5d).
 279 Moreover, flight type was also associated with temperature ($\chi^2_6 = 40.8^{***}$) and wind
 280 speed ($\chi^2_6 = 56.9^{***}$) (Appendix H.1).

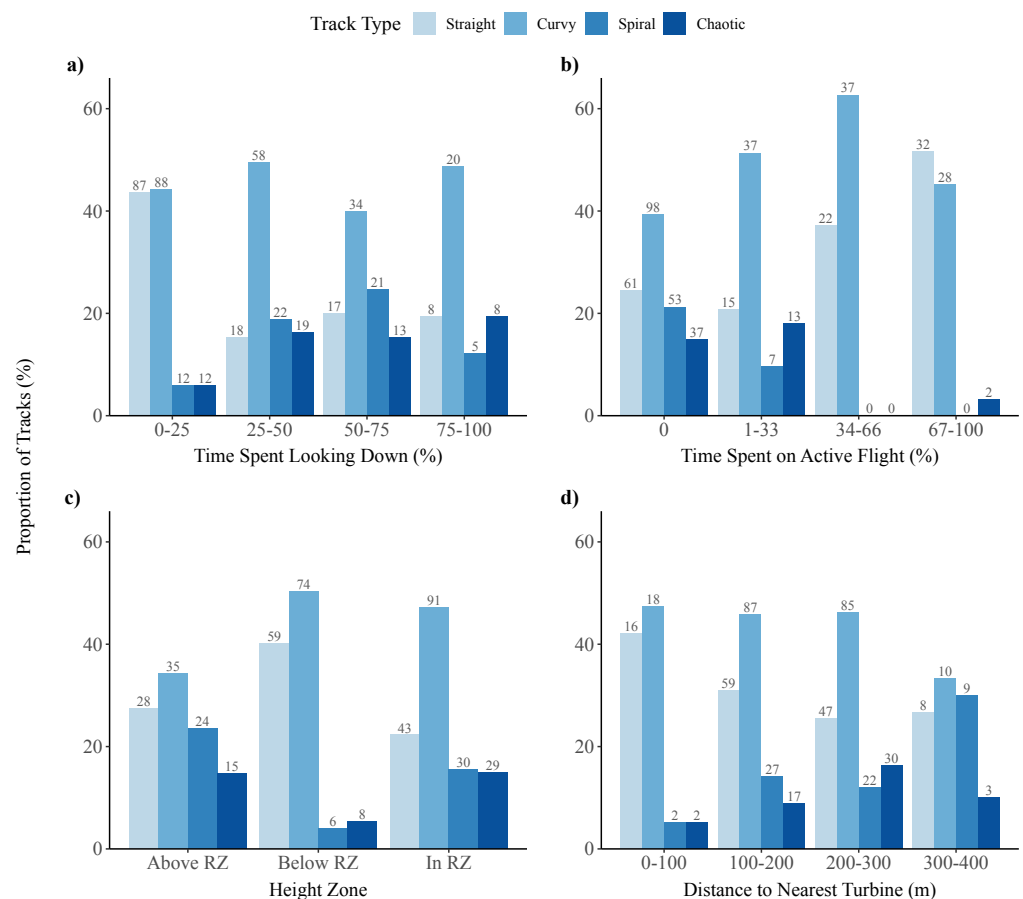


Figure 5. Proportion of occurrences of each track type in relation to (a) the proportion of time the birds spent looking down, (b) the proportion of time spent on active flight, (c) flight altitude divided into groups based on the rotor zone (RZ) of the nearest turbine and (d) the distance of the nearest turbine. The number of tracks is annotated above each bar.

281 Flight altitude was negatively correlated with wind speed ($r_s = -0.370^{***}$) and
 282 it was found that raptors flew at lower altitudes with increasing wind speeds (Figure
 283 6). When assessing this correlation for each track type individually, it was found that

284 this association was strongest for individuals flying in curvy patterns ($r_s = -0.470^{***}$).
285 Correlations were also found between flight altitude and cloud coverage ($r_s = 0.0349^{**}$)
286 and temperature ($r_s = 0.0833^{***}$), however these correlations were weaker than that of
287 wind speed (Appendix H.2).

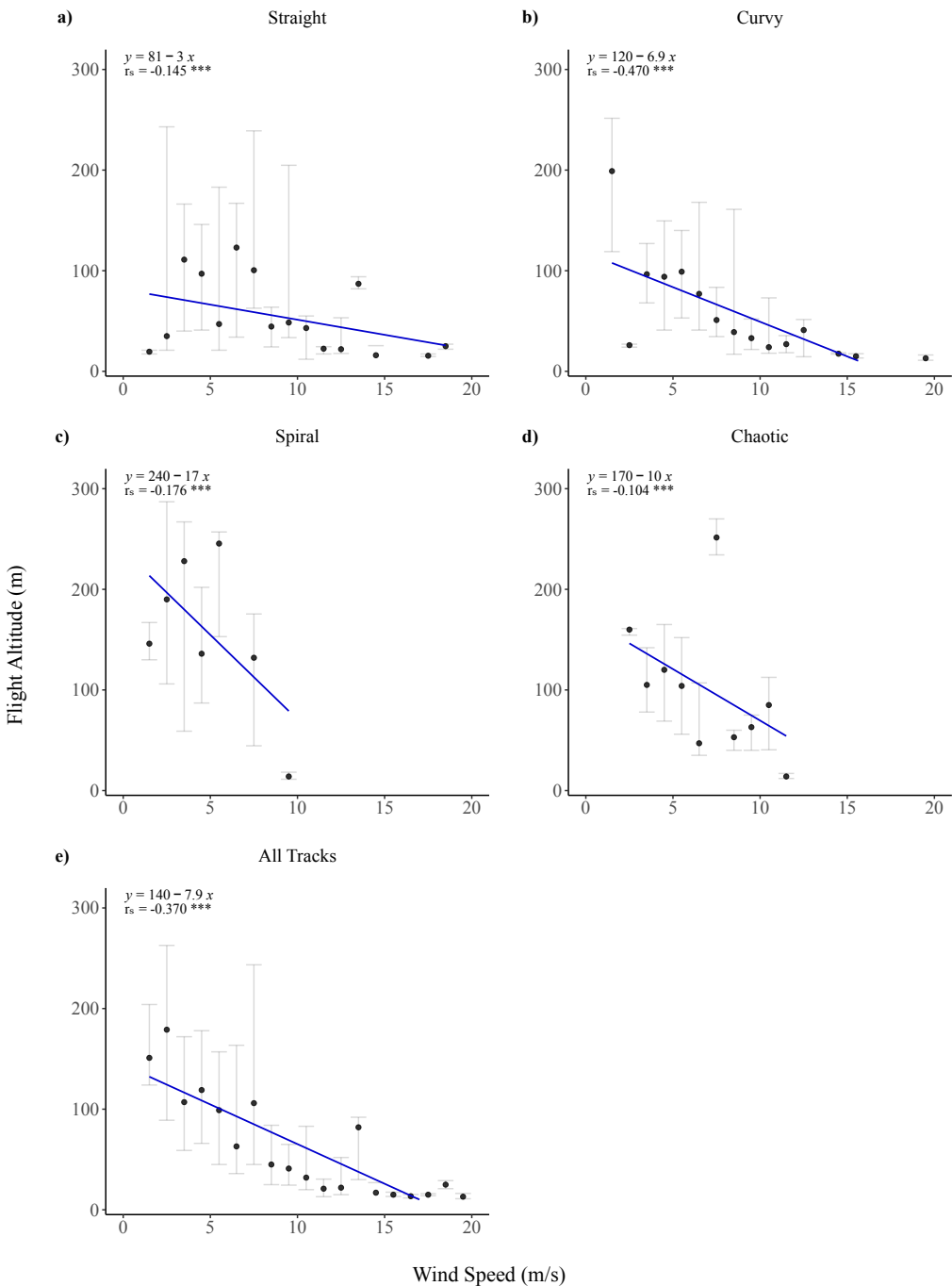


Figure 6. Linear regression of flight altitude above ground level in relation to wind speed, (a–d) grouped by track type and for (e) all track types collectively. For each regression, the median flight altitude was used for each m/s. The regression equation and correlation coefficient (r_s) is given for each plot. The horizontal bars represent the variance around each median (IQR).

288 A significant positive correlation ($r_s = 0.309^{***}$) was found between time spent
289 looking down and flight asymmetry (sum of directional changes) (Figure 7a). Showing
290 that when their flight path was less symmetrical raptors spent more time looking down,
291 i.e. the more asymmetrical their flight path was the less vigilant they were. Furthermore,

for individuals in active flight the relationship between time spent looking down and flight asymmetry was more positively correlated ($r_s = 0.426^{***}$) (Appendix H.3). Time spent looking down was negatively correlated ($r_s = -0.310^{***}$) with track length ratio, indicating that raptors with a more direct path also were the most vigilant (Figure 7b). Time spent looking down was also found to be negatively correlated ($r_s = -0.427^{***}$) with time spent on active flight, meaning that raptors actively flying were more vigilant (Figure 7c). A significant positive correlation was also found between time spent looking down and flight altitude ($r_s = 0.135^{***}$). However, when looking at this relationship for each track type individually, it was only straight tracks that also showed a significant positive correlation ($r_s = 0.208^{***}$). For chaotic tracks this correlation was negative ($r_s = 0. -149^*$) and no significant correlation was found for the two other track types (Appendix H.4).

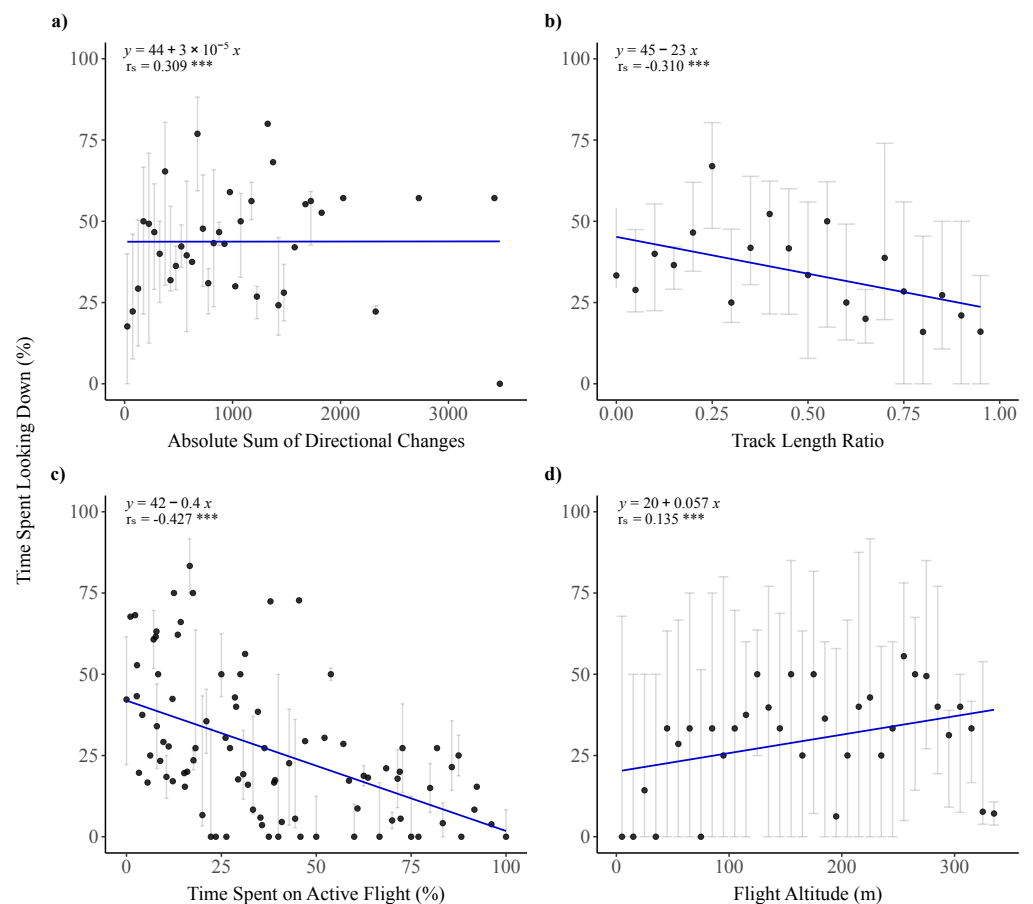


Figure 7. Linear regression of the proportion of time each individual spent looking down in relation to (a) the sum of directional changes, (b) the track length ratio, (c) the proportion of time spent on active flight, and (d) flight altitude. For each regression, the median proportion of time spent looking down was used for each corresponding variable (every 50 sum of directional changes; each 0.05 ratio value; each % for active flight; and every 10 m). The regression equation and correlation coefficient (r_s) is given for each plot. The horizontal bars represent the variance around each median (IQR).

3.2. Avoidance Behavior

A weak correlation was found between distance to nearest turbine and flight altitude for all track types ($r_s = 0.0658^{***}$; Figure 8). When grouping the tracks by type a slightly larger positive correlation was found for the track types curve ($r_s = 0.110^{***}$), and spiral ($r_s = 0.134^{***}$), whereas for chaotic tracks this correlation was negative ($r_s = -0.0854^{**}$) and for straight tracks this correlation was not significant ($p > 0.05$).

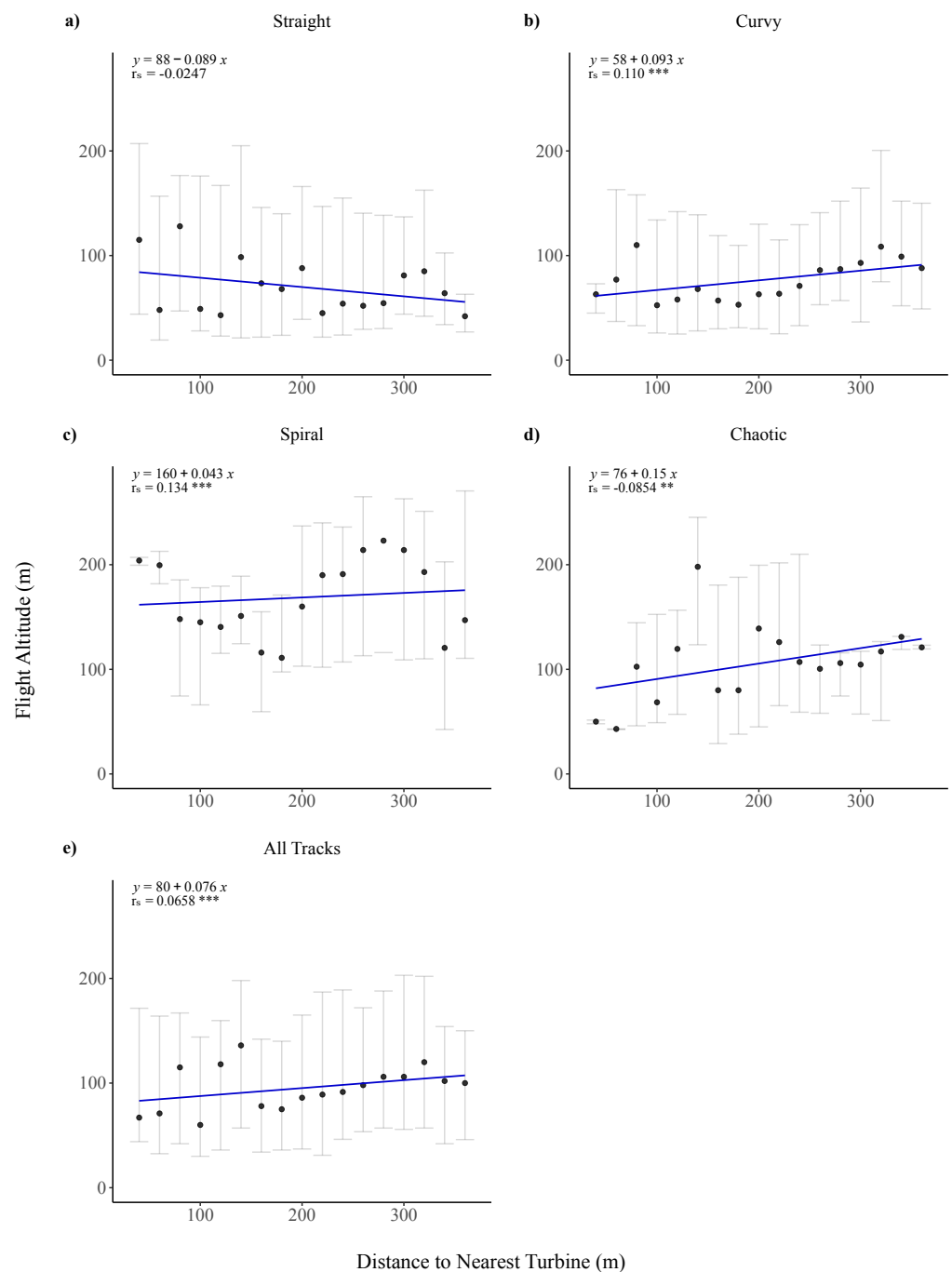


Figure 8. Linear regression of distance to the nearest turbine in relation to flight altitude above ground level, (a–d) grouped by track type and for (e) all track types collectively. For each regression, the median flight altitude was used for every 20 m. The regression equation and correlation coefficient (r_s) is given for each plot. The horizontal bars represent the variance around each median (IQR).

When comparing the relationship between flight altitude and time spent looking down for raptors in close proximity to a turbine with those distant to a turbine, positive correlations were found at both distances (close: $r_s = 0.219$ ***; distant: $r_s = 0.177$ ***), but the slope of the regression trend line for raptors in close proximity was a fivefold larger than that of distant raptors (Figure 9). Hence, individuals in close proximity to the nearest wind turbine clearly flew at higher altitudes if spending a larger amount of time looking down.

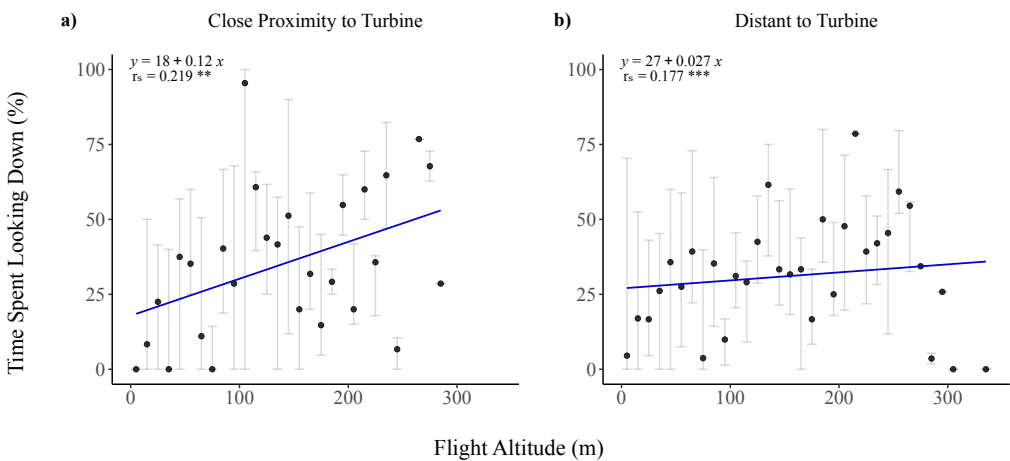


Figure 9. Linear regression of the proportion of time each individual spent looking down in relation to flight altitude above ground level, grouped by distance to nearest turbine **(a)** close: <150 m and **(b)** distant: >150 m. For each regression, the median proportion of time spent looking down was used for every 10 m. The regression equation and correlation coefficient (r_s) is given for each plot. The horizontal bars represent the variance around each median (IQR).

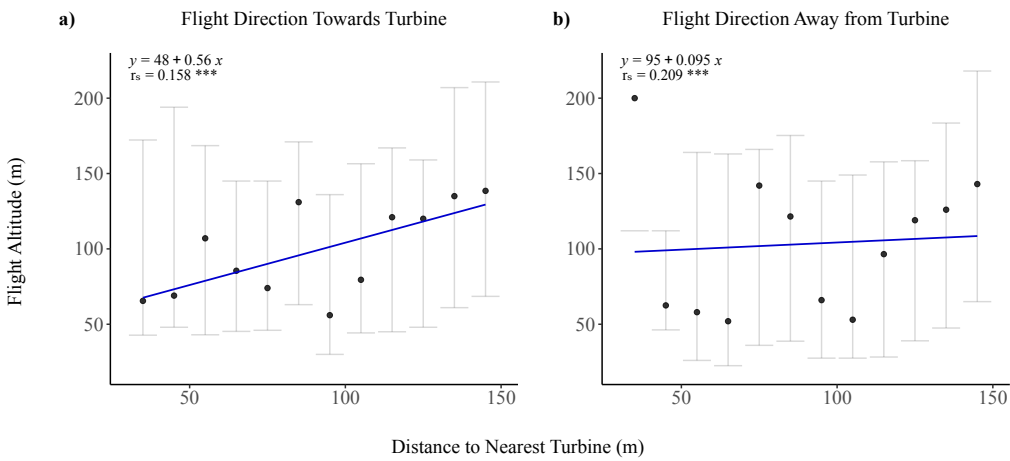


Figure 10. Linear regression of distance to the nearest turbine (<150 m) in relation to flight altitude above ground level grouped by flight direction **(a)** flying towards the nearest turbine and **(b)** flying away from the nearest turbine. For each regression, the median flight altitude (m) was used for every 10 m. The regression equation and correlation coefficient (r_s) is given for each plot. The horizontal bars represent the variance around each median (IQR).

317 For raptors in close proximity to the nearest turbine (<150 m) a significant positive
318 correlation was found between distance to the nearest turbine and flight altitude when
319 raptors were flying towards the nearest turbine ($r_s = 0.158^{***}$) and a slightly stronger
320 correlation was found when raptors flying away from the nearest turbine ($r_s = 0.209^{***}$)
321 (Figure 10). When raptors were flying towards a turbine, a positive correlation was
322 found between distance to nearest turbine and time spent looking down for all three
323 altitude zones separately (above: $r_s = 0.126^{***}$; below: $r_s = 0.147^{***}$; in: $r_s = 0.0789^{*}$)
324 (Figure 11).

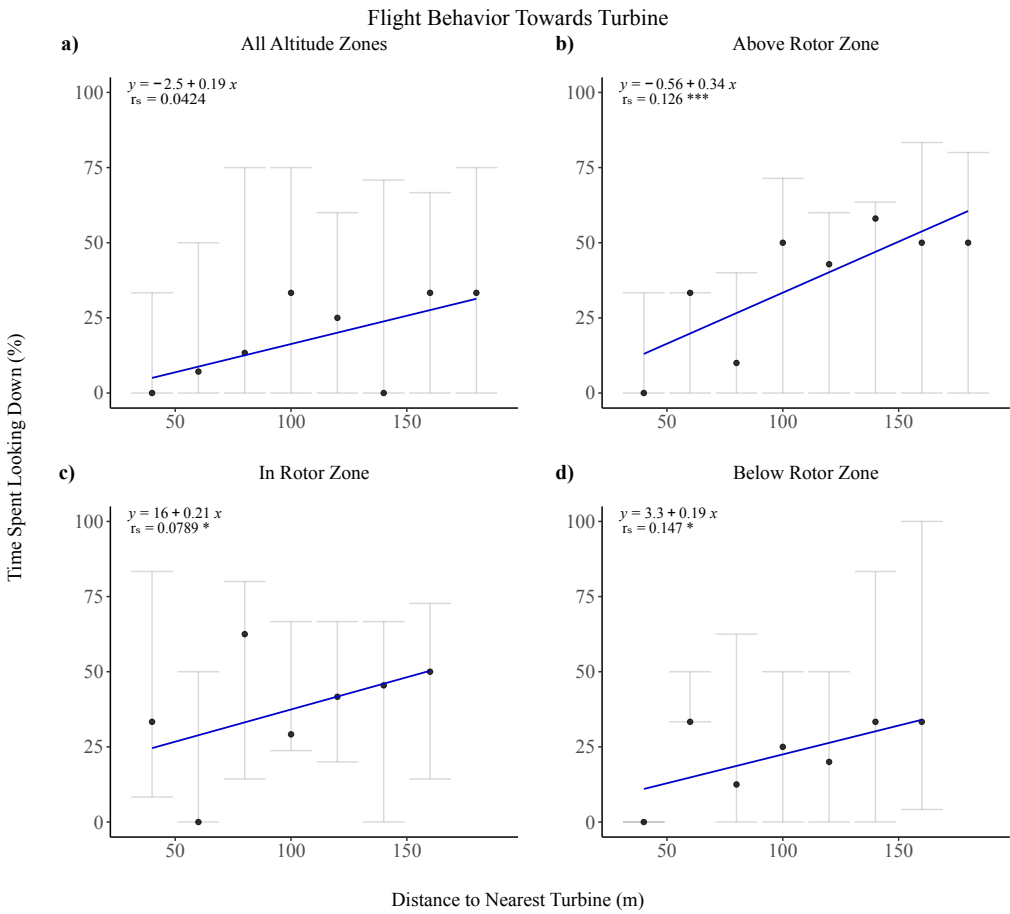


Figure 11. Linear regression, for individuals flying towards a turbine, of the proportion of time the birds spent looking down for each track (median values for turbine distance groups per 20 m) in relation to distance of the nearest turbine. The linear regression models were also made for tracks divided into groups based on the rotor zone of the nearest turbine. The regression equation and correlation coefficient (r_s) is given for each plot. The horizontal bars represent the variance around each median (IQR).

4. Discussion

4.1. Flight Behavior Described by Flight Trajectories and Flight Orientation

The results of the case study demonstrate how flight trajectories can be used to describe flight behavior by classifying track type. Moreover, the absolute sum of track angles and the track length ratio can be used to quantitatively assess risk prone behavior. Flight symmetry, quantified by the absolute sum of track angles, can be used to describe flight behavior, showing that tracks with low tortuosity i.e. straight and curvy tracks also were the most symmetrical tracks and the most asymmetrical tracks were those with high tortuosity i.e. spiral and chaotic tracks (Figure 3). Track length ratio proved to be a robust indication of tortuosity, showing that individuals with straight flight types also had the highest length ratio i.e. essentially flying in the most direct path (Figure 4). Previous studies have often described tortuosity as an indicator for collision risk, hypothesizing birds with a more tortuous flight path to be at higher risk for collision [6,33,34]. The inference of these studies is based on the expectation that a more tortuous flight path is associated with a larger amount of time flying and when flying there will always be a collision risk. Furthermore, the results in this study found a significant positive correlation between time spent looking down and flight asymmetry and a significant negative correlation between time spent looking down and track length ratio, both indicating that individuals with a more tortuous flight behavior are less vigilant

(Figure 5a and Figure 7a–b), hence supporting the hypothesis that birds with a tortuous flight path are at increased risk for collision.

The time individuals spent looking down was found to be significantly negatively correlated with time spent on active flight, i.e. individuals utilizing active flight methods were more vigilant (Figure 7b). Individuals that spent a greater amount of time on active flight also generally had a more direct flight path, as individuals flying in a chaotic or spiral flight pattern generally spent a small proportion of time on active flight (Figure 5b). Thus, indicating that these flight types are more reliant on soaring to increase altitude. Furthermore, the results clearly show that the use of thermal soaring lead to spiral flight patterns, as it was found that individuals flying in spiral patterns occurred more frequently at temperatures above 10 °C and low wind speeds (Appendix H.1). These findings are in agreement with the expectation that weather variables affect flight behavior, more particularly the utilization of thermal soaring.

Another important predictor of collision risk is flight altitude in relation to the rotor zone i.e. flight in the rotor zone is associated with a higher collision risk [6,9,33–35]. Flight altitude has previously been found to be determined by movement type e.g. migratory or local movement [6]. Lanzone *et al.* [6] and Bergen *et al.* [34] found that migratory birds flying in a linear fashion flew at higher altitudes. Contrary to this, the results in this study show that most individuals flying in straight (or curvy) patterns flew at altitudes in or below the rotor zone (Figure 5c). These contradicting results are however likely to be due to the raptors on Gotland mainly consisting of breeding populations, as the island is not directly part of any migratory routes for these species [26]. The raptors in this study are therefore assumed to be mainly local birds. Similar to the findings in this study, Dahl *et al.* [14] found that occurrences below the rotor zone were mainly individuals engaging in directional flight and some engaging in social behavior. Moreover, distance to wind turbines is an obvious predictor of collision risk. In this study it was found that most of the raptors flying near turbines had the flight type straight or curvy and that the proportion of raptors flying in a spiral or chaotic pattern increased with distance to the nearest turbine. This is in agreement with previous studies showing that soaring birds change their flight trajectories to avoid wind turbines [3,10,13].

4.1.1. Effect of Weather on Flight Behavior

Understanding how weather affects flight behavior is important for developing risk assessment models. In this study a significant negative correlation was found between flight altitude and wind speed i.e. the raptors flew at lower altitudes with increasing wind speeds (Figure 6). In accordance with these findings previous studies also found that eagles were more likely to fly at altitudes under 150 meters at higher wind speeds [35,36]. Kuehn *et al.* [35] suggests that these results reflect an increasing collision risk at higher wind speeds. Contrary to this, we suggest that, while moderate wind speeds (5–10 m/s) result in an increased collision risk, due to the resulting flight altitudes being within the rotor zone, high wind speeds (>10 m/s) generally result in flight altitudes below the rotor zone and the risk of collision with moving rotor blades is therefore negligible (Figure 6).

4.2. Avoidance Behavior

The findings of the case study prove the use of variables describing flight behavior and thereby camera-based monitoring systems such as IdentiFlight for evaluating avoidance behavior, as the results indicate that golden eagles, white-tailed eagles and red kites exhibit some degree of meso-avoidance to the turbines within the wind farm on Gotland. Most previous studies show that raptors exhibit avoidance behavior by increasing flight altitude in proximity to turbines [9,11,15,18,22]. In this study the species studied decreased flight altitude in proximity to turbines. This response is also an indication of avoidance behavior, as it can be argued that avoidance also can take place

under the rotor zone. This avoidance response becomes more evident when dividing the track types according to flight direction (Figure 10). This avoidance response may be explained as when nearing a turbine the use various flight methods to increase altitude is reduced. Furthermore, it was found that individuals in close proximity to the nearest wind turbine flew at higher altitudes if spending a larger amount of time looking down (Figure 9a). Thus, individuals foraging increase their altitude to increase time spent looking down to forage, indicating even foraging individuals, which are expected to be less vigilant, display avoidance behavior to turbines. Moreover, when comparing the avoidance behavior of individuals oriented towards the nearest turbine when flying either above, below or in the rotor zone, towards a turbine a positive correlation was found, between distance to nearest turbine and time spent looking down, for all three altitude zones. While this correlation was largely similar for individuals flying at altitudes above or below the rotor zone, the correlation was weaker for individuals flying towards the turbine at altitudes within the rotor zone. (Figure 11). This could indicate that individuals flying at altitudes within the rotor zone exhibit a lower avoidance behavior and are at a larger risk for colliding with the turbine.

5. Conclusion

To our knowledge this is the first study providing robust quantitative results describing raptors’ flight behavior. Our findings on flight behavior have previously been described in theory, but the results presented in this study are the first to demonstrate this theoretical knowledge with comprehensive measurable results. Furthermore, this study provides a framework for future research, using data from camera-based monitoring systems, demonstrating how flight trajectories and bird images can be utilized to describe risk prone behavior and thereby assess collision risk and avoidance behavior. Thus, providing a crucial step towards quantifying collision risk to be used in future predictive models. However, this study is only based on assumptions that behaviors such as foraging and tortuous flight are more prone to collision. It is therefore necessary to assess the behavior of individuals hit by turbines prior to the collision. The use of camera-based monitoring systems along with a collision detecting system such as the WT-Bird system, that can detect collisions through the use of acoustic sensors on turbine blades [37] would enable the necessary data to be collected. This study provides a quantitative method that can be utilized to analyze such data and factually determine which behaviors lead to an increased collision risk.

Author Contributions: Conceptualization, A.C.L., B.L., C.P., D.B. and H.L.; methodology, A.C.L., B.L., C.P., D.B. and H.L.; formal analysis, A.C.L. and H.L.; investigation, A.C.L. and H.L.; resources, B.L.; data curation, A.C.L. and H.L.; writing—original draft preparation, A.C.L. and H.L.; writing—review and editing, A.C.L., B.L., C.P., D.B. and H.L.; visualization, A.C.L. and H.L.; supervision, B.L., C.P. and D.B. All authors have read and agreed to the published version of the manuscript.

Funding: This research received no external funding.

Data Availability Statement: The data presented in this study are available on request from the corresponding author.

Acknowledgments: Special thanks to Tyler Derritt and the rest of the IdentiFlight team for technical assistance.

Conflicts of Interest: The authors declare no conflict of interest.

440 **Appendix A. Study Site**



Figure A.1. The IDF Tower (red drop) and the 400 meters zone (orange circle) around the tower i.e. the observational zone. The wind turbines that the birds within the 400 meters zone flew closest to (orange crosses) and other turbines (grey crosses) within the wind farm.

441 **Appendix B. Operational Days**

Table B.1. Number of days where the camera system were operational, number of days with sightings of the selected raptor species (red kite, golden eagle, and white-tailed eagle), and number of tracks for each month.

Month	Operational days	Days with raptors	Number of tracks
February	20	14	53
March	31	25	153
April	30	23	91
May	31	20	69
June	12	8	8
July	11	6	20
August	18	16	87
September	30	23	140
October	26	13	39
November	22	5	12
Total	231	153	672

442 **Appendix C. IdentiFlight System**

443 *Appendix C.1. Curtailment Prescription*

Table C.1. Model type, number of turbines, rotor diameter, hub height, rotor zone, radius of outer and inner cylinder, and height of outer and inner cylinder for covered and partially covered wind turbines.

Model	Number of turbines	Rotor diameter (m)	Hub height (m)	Rotor zone (m above ground level)	Radius of outer cylinder (m)	Radius of inner cylinder (m)	Height of outer cylinder (m)	Height of inner cylinder (m)
Covered								
Vestas V27	1	27	31	15.5–46.5	700	250	300	200
Vestas V29	1	29	31	14.5–47.5	700	250	300	200
Vestas V90	1	90	80	33–127	700	400	400	250
Partially covered								
Kenersys 2500 100	1	100	85	33–137	600	300	400	250
Vestas V47	2	47	45	19.5–70.5	600	300	300	200
Vestas V90	2	90	80	33–127	700	300	400	250
Vestas V100	1	95	100	50.5–149.5	700	400	400	250

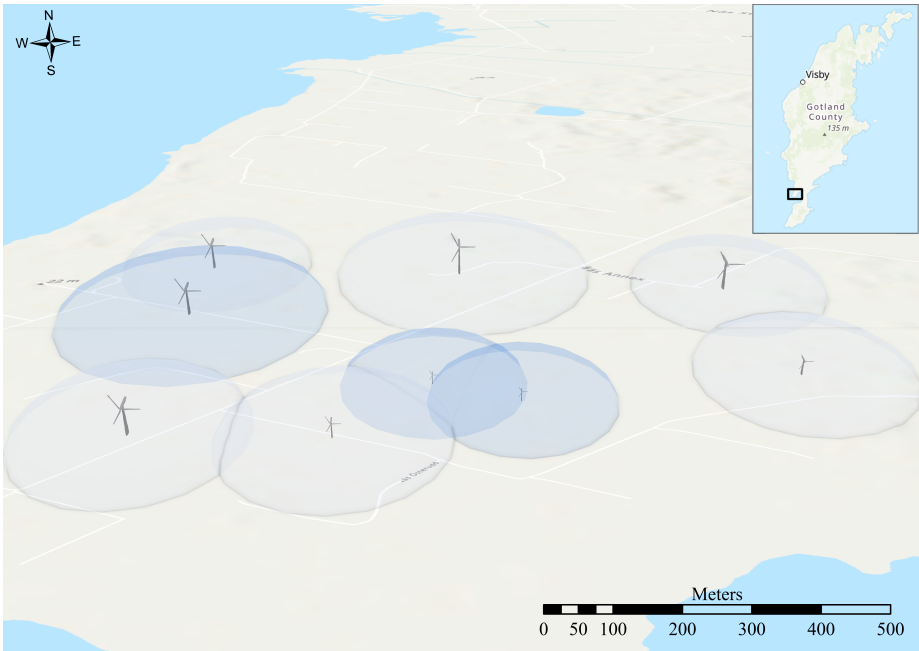


Figure C.1. Fully covered (dark blue) and partially covered (light blue) wind turbines by the IDF tower. The horizontal curtailment zone (radius of inner cylinder) is shown around each turbine.

444 *Appendix C.2. IdentiFlight Camera System*



Figure C.2. IdentiFlight tower at study site.

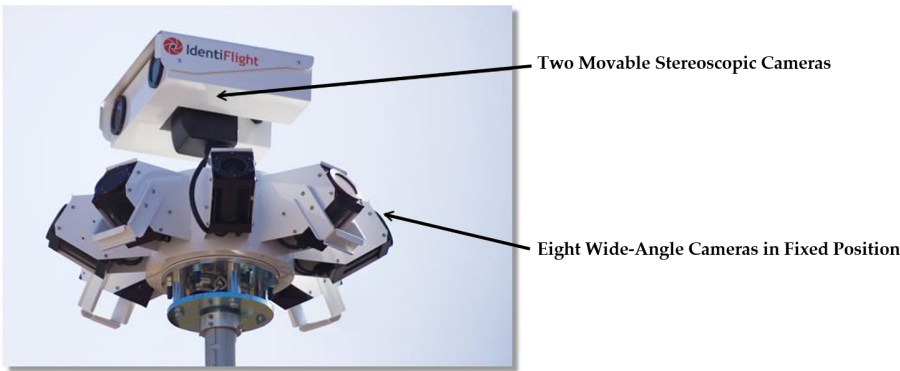


Figure C.3. Imaging head components of the IdentiFlight tower. The bottom part consist of eight fixed cameras that can detect eagle sized objects and separate important from unimportant motion of birds. When important motion is detected the top part tracks that bird as it consist of two movable cameras, that also measure the distance of the the bird it is tracking [27].

445 **Appendix D. IdentiFlight Data**

446 The IDF system registers a large variety of variables for each observation of each
447 track (Figure D.1). Whenever a bird of interest is detected it is assigned an unique track
448 ID that is used for all observations of that bird. For each observation a image is taken of
449 the bird at that specific time, as the system notes the time and date. Furthermore, the
450 longitude and latitude as well as the height above ground level is registered, which gives
451 multiple GPS coordinates of each bird i.e. tracks. Horizontal distance between the bird
452 and camera tower as well as the distance between the bird and nearest turbine is also
453 registered for each observation. Moreover, the system determines the species of each
454 bird and gives a confidence level of the species classification. The system can classify a
455 bird in the following categories: eagle, white-tailed eagle, golden eagle, non eagle, red
456 kite, red or black kite, buzzard, gull, and other avian species.


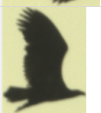

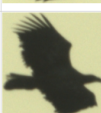
	A	B	C	D	E	F	G	H	I	J	K			
1	TrackID	DateTimeStamp	Latitude	Longitude	Species	Type	Name	Confidence	Level	HeightAGL_m	HorizontalDistance_m	ClosestTurbine	TurbineDistance_m	Image
2	bb44b6a4-0516-4777-a782-76cf0a97d3	2-17-2020 9:57:29.099	57.0682041	18.21678264	EAGLE			0.899		10	280.316		62.32716662	
3	bb44b6a4-0516-4777-a782-76cf0a97d3	2-17-2020 9:57:30.104	57.0682913	18.21666061	EAGLE			0.92		12	268.316		52.75143125	
4	bb44b6a4-0516-4777-a782-76cf0a97d3	2-17-2020 9:57:32.106	57.0683501	18.21647471	EAGLE			0.92		9	257.316		43.38468737	
5	bb44b6a4-0516-4777-a782-76cf0a97d3	2-17-2020 9:57:33.111	57.0683494	18.21644777	EAGLE			0.92		8	256.316		42.40242798	

Figure D.1. Example of data output given by the IdentiFlight system.

457 **Appendix E. Subsets**

Table E.1. Number of observations and tracks for each data set and each subset based on track type, distance to turbine and altitude zone, respectively. For analyses containing all tracks and the variables, % time looking down and active flight, the data set ≥ 100 m & ≥ 4 images was used. Otherwise the dataset the ≥ 100 m was used for analyses with all tracks. Tracks with odd deviations were removed from all data sets. For the subset dividing observations by altitude zone only observations within 180 meters of the nearest turbine were used.

	Observations	Tracks
All tracks		
≥ 100 m	8036	564
≥ 100 m & ≥ 4 images	7796	442
Divided by track type		
Straight	1418	130
Curvy	3190	200
Spiral	1892	60
Chaotic	1296	52
Divided by distance to turbine		
Close	2215	148
Distant	5826	348
Divided by altitude zone		
Above rotor zone	1311	256
Below rotor zone	820	236
In rotor zone	1580	320

Appendix F. Calculations

Appendix F.1. Track Length Ratios

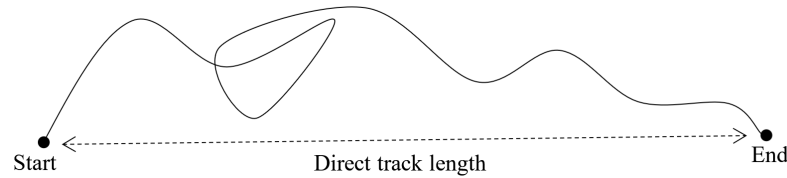


Figure F.1. Model of a track, showing the direct track length (the dotted arrow) in comparison to the actual track length.

The track length ratio was calculated for each track as shown in Equation A1, where the direct track length is the shortest distance from a track's start point to the track's end point (Figure F.1). This resulted in a measure of deviations from the most direct path, where a value of 1 represents a flight path with no deviations. The smaller the value the more deviations from the direct flight path.

$$\text{Track length ratio} = \frac{\text{Direct track length}}{\text{Actual track length}} \quad (\text{A1})$$

Appendix F.2. Track Angles

A track is based on the observations of a single individual i.e. multiple points that are connected in a chronological order. When an individual turns it will be seen as an angle in the connected points. Left turns and right turns were distinguish as the track angles ranged from -180° to 180° (figure F.2).

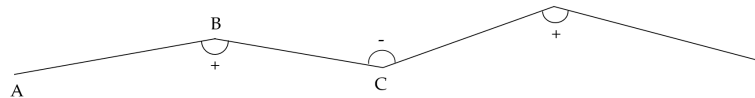


Figure F.2. Model of a track. Right turns ranged from 0 to 180° and left turns from -180 to 0° , which are annotated with $+$ and $-$, respectively. Trigonometry was used to calculate the angles therefore three points was used to calculate each angle e.g. when calculating the angle for the point B the points A and C was used as well.

To calculate the angles of the track the inverse trigonometric function of cosine (arccos) was used as shown in Equation A2. A, B and C represents points as shown in Figure F.2, where AB is the distance from point A to point B, and BC is the distance between point B and C and so on.

$$\angle B = \arccos\left(\frac{AB^2 + BC^2 - AC^2}{2 \cdot AB \cdot BC}\right) \quad (\text{A2})$$

The absolute sum of track angles was calculated for each track as shown in Equation A3. This resulted in a measure of flight symmetry, where a value of 0 represents a perfectly symmetrical track in terms of the number of turns and the size of them to the left and to the right. The larger the value the more asymmetrical the track in relation to turns to either the left or the right.

$$\text{Absolute Sum of } \angle = \left| \sum_{i=1}^n \angle_i \right| \quad (\text{A3})$$

479 **Appendix G. χ^2 Contingency Test**

Table G.1. χ^2 contingency test for the proportion (%) of each track type (straight, curvy, spiral, and chaotic) in relation to time spent looking down, distance to nearest turbine, height zone (in, below, and above rotor zone), active flight and the three different weather variables; wind speed, temperature, and cloud coverage. Significant results are annotated with *.

	Time spent looking down (%)	Distance to nearest turbine (m)	Height zone	Proportion of time on active flight (%)	Wind speed (m/s)	Temperature (°C)	Cloud coverage (%)
χ^2	55.8***	18.6*	38.2***	65.3***	56.9***	40.8***	12.1
df	9	9	6	9	6	6	6

480 **Appendix H. Supplementary Results**

481 *Appendix H.1. Track Types in Relation to Weather*

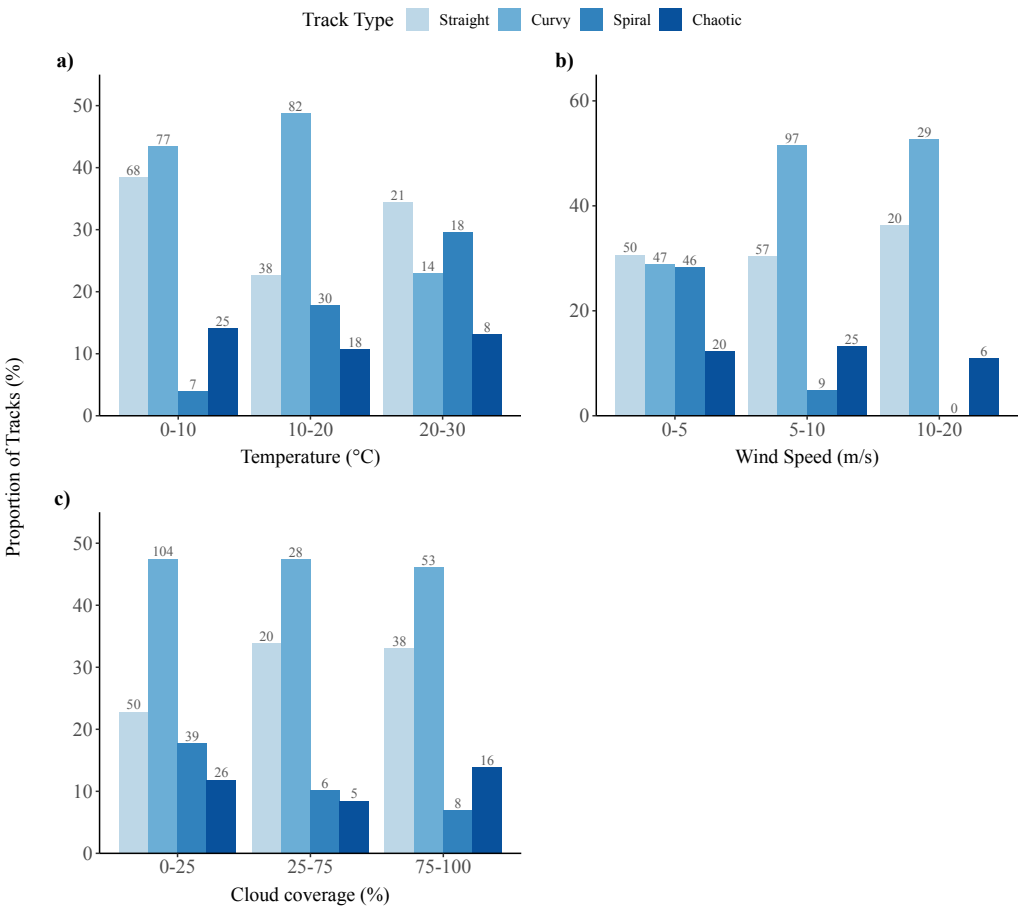


Figure H.1.1. Proportion of occurrences of each track type in relation to wind speed, temperature, and cloud coverage, respectively. The number of tracks is annotated above each bar.

482 *Appendix H.2. Flight Altitude in Relation to Weather*

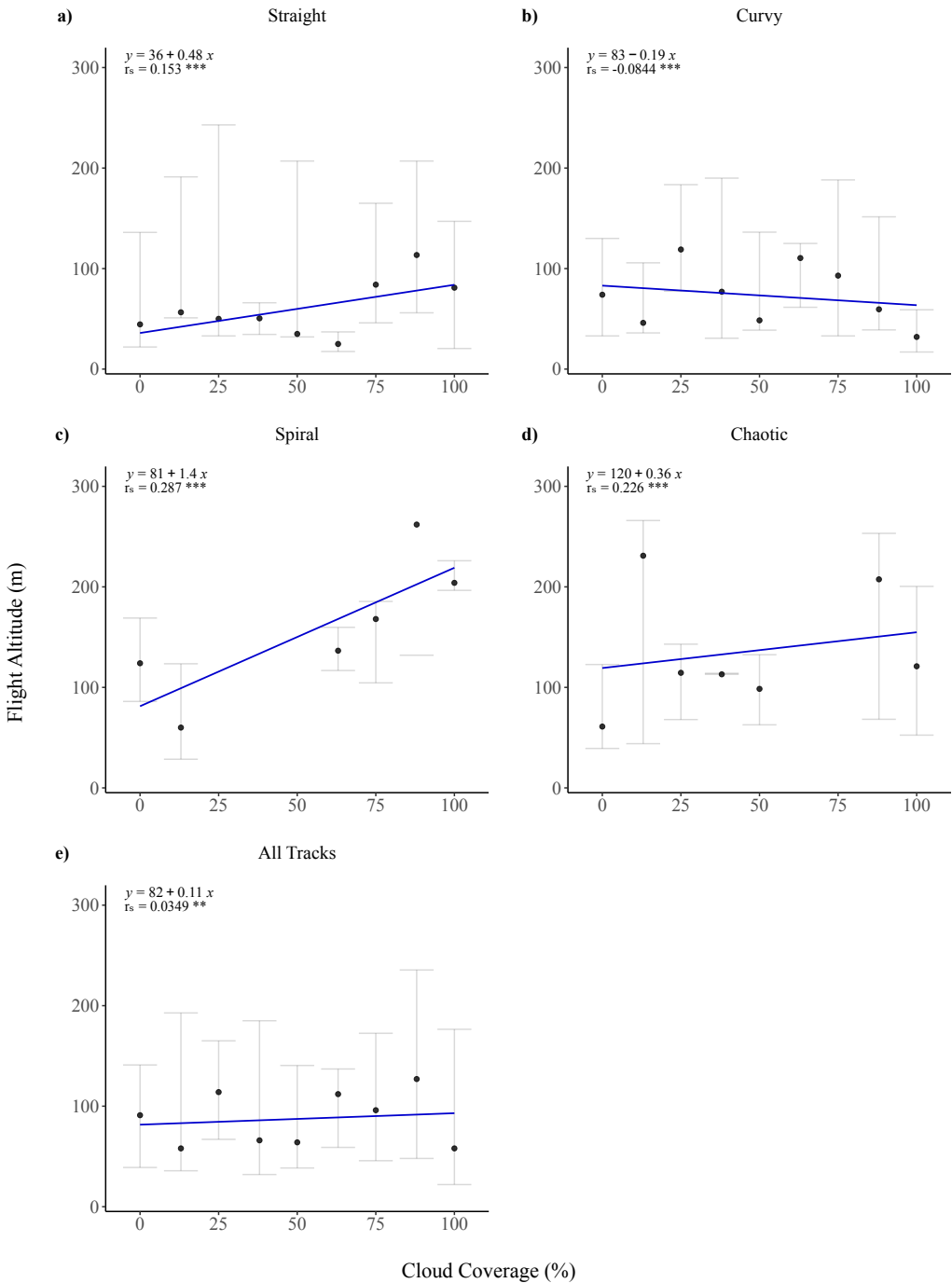


Figure H.2.1. Linear regression of flight altitude above ground level in relation to cloud coverage, (a–d) grouped by track type and for (e) all track types collectively. For each regression, the median flight altitude was used for each % cloud coverage. The regression equation and correlation coefficient (r_s) is given for each plot. The horizontal bars represent the variance around each median (IQR).

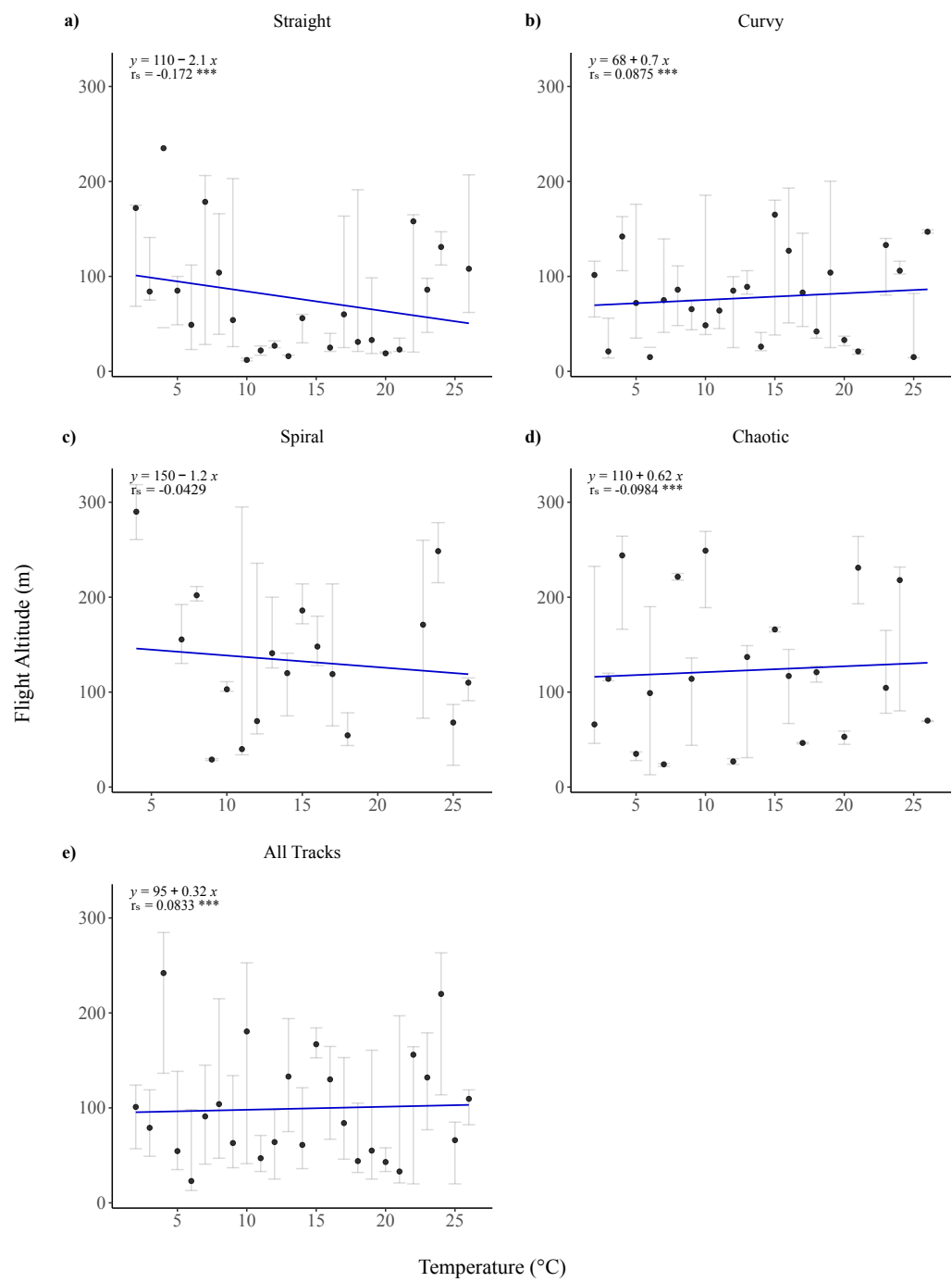


Figure H.2.2. Linear regression of flight altitude above ground level in relation to temperature, (a–d) grouped by track type and for (e) all track types collectively. For each regression, the median flight altitude was used for each °C. The regression equation and correlation coefficient (r_s) is given for each plot. The horizontal bars represent the variance around each median (IQR).

483 *Appendix H.3. Flight Behavior of Individuals in Active Flight*

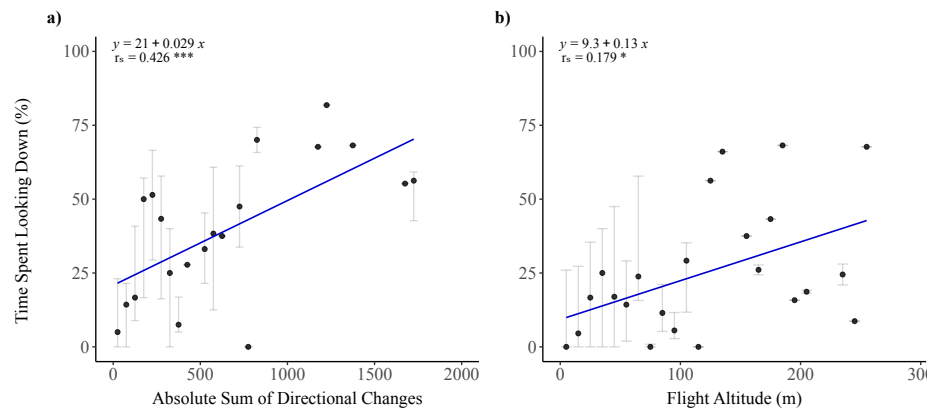


Figure H.3.1. Linear regression, for individuals in active flight, of the proportion of time each individual spent looking down in relation to (a) the sum of directional changes, and (b) flight altitude above ground level. For each regression, the median proportion of time spent looking down was used for each corresponding variable (every 200 sum of directional changes; and every 10 m for flight altitude). The regression equation and correlation coefficient (r_s) is given for each plot. The horizontal bars represent the variance around each median (IQR).

484 *Appendix H.4. Vigilance*

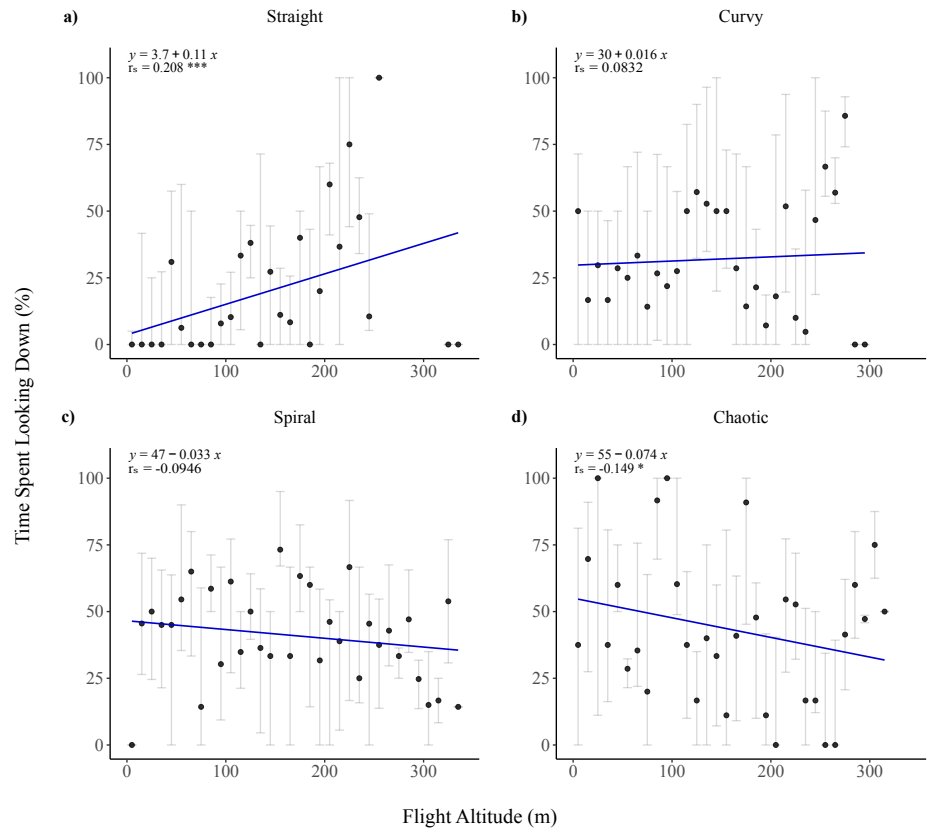


Figure H.4.1. Linear regression of the proportion of time each individual spent looking down in relation to flight altitude above ground level, grouped by track type. For each regression, the median proportion of time spent looking down was used for every 10 m. The regression equation and correlation coefficient (r_s) is given for each plot. The horizontal bars represent the variance around each median (IQR).

References

1. Drewitt, A.L.; Langston, R.H.W. Assessing the Impacts of Wind Farms on Birds. *Ibis* **2006**, *148*, 29–42. doi:10.1111/j.1474-919X.2006.00516.x.
2. Madders, M.; Whitfield, D.P. Upland Raptors and the Assessment of Wind Farm Impacts. *Ibis* **2006**, *148*, 43–56. doi:10.1111/j.1474-919X.2006.00506.x.
3. de Lucas, M.; Janss, G.F.E.; Whitfield, D.P.; Ferrer, M. Collision Fatality of Raptors in Wind Farms does not Depend on Raptor Abundance. *Journal of Applied Ecology* **2008**, *45*, 1695–1703. doi:10.1111/j.1365-2664.2008.01549.x.
4. Smallwood, K.S.; Thelander, C. Bird Mortality in the Altamont Pass Wind Resource Area, California. *The Journal of Wildlife Management* **2008**, *72*, 215–223. doi:10.2193/2007-032.
5. Bevanger, K.; Berntsen, F.; Clausen, S.; Dahl, E.L.; Flagstad, Ø.; Follestad, A.; Halley, D.; Hanssen, F.; Johnsen, L.; Kvaløy, P.; Lund-Hoel, P.; May, R.; Nygård, T.; Pedersen, H.C.; Reitan, O.; Røskift, E.; Steinheim, Y.; Stokke, B.; Vang, R. *Pre- and Post-construction Studies of Conflicts Between Birds and Wind Turbines in Coastal Norway (Bird-Wind). Report on Findings 2007-2010*, 2010.
6. Lanzone, M.; Maisonneuve, C.; Tremblay, J.A.; Mulvihill, R.; Jr, G.T.M. Topography Drives Migratory Flight Altitude of Golden Eagles: Implications for On-Shore Wind Energy Development. *Journal of Applied Ecology* **2012**, *49*, 1178–1186. doi:10.1111/j.1365-2664.2012.02185.x.
7. Loss, S.R.; Will, T.; Marra, P.P. Estimates of Bird Collision Mortality at Wind Facilities in the Contiguous United States. *Biological Conservation* **2013**, *168*, 201–209. doi:10.1016/j.biocon.2013.10.007.
8. May, R.; Hoel, P.L.; Langston, R.; Dahl, E.L.; Bevanger, K.; Reitan, O.; Nygård, T.; Pedersen, H.C.; Røskift, E.; Stokke, B.G. *Collision Risk in White-tailed Eagles. Modelling Collision Risk using Vantage Point Observations in Smøla Wind-power Plant*, 2010.
9. Garvin, J.C.; Jennelle, C.S.; Drake, D.; Grodsky, S.M. Response of Raptors to a Wind farm. *Journal of Applied Ecology* **2011**, *48*, 199–209. doi:10.1111/j.1365-2664.2010.01912.X.
10. Barrios, L.; Rodríguez, A. Behavioural and Environmental Correlates of Soaring-bird Mortality at On-shore Wind Turbines. *Journal of Applied Ecology* **2004**, *41*, 72–81. doi:10.1111/j.1365-2664.2004.00876.x.
11. Johnston, N.N.; Bradley, J.E.; Otter, K.A. Increased Flight Altitudes Among Migrating Golden Eagles Suggest Turbine Avoidance at a Rocky Mountain Wind Installation. *PloS one* **2014**, *9*, e93030. doi:10.1371/journal.pone.0093030.
12. Murgatroyd, M.; Photopoulou, T.; Underhill, L.G.; Bouten, W.; Amar, A. Where Eagles Soar: Fine-Resolution Tracking Reveals the Spatiotemporal Use of Differential Soaring Modes in a Large Raptor. *Ecology and Evolution* **2018**, *8*, 6788–6799. doi:10.1002/ece3.4189.
13. Marques, A.T.; Santos, C.D.; Hanssen, F.; Muñoz, A.; Onrubia, A.; Wikelski, M.; Moreira, F.; Palmeirim, J.M.; Silva, J.P. Wind Turbines Cause Functional Habitat Loss for Migratory Soaring Birds. *Journal of Animal Ecology* **2019**, *89*, 93–103. doi:10.1111/1365-2656.12961.
14. Dahl, E.L.; May, R.; Hoel, P.L.; Bevanger, K.; Pedersen, H.C.; Røskift, E.; Stokke, B.G. White-Tailed Eagles (*Haliaeetus albicilla*) at the Smøla Wind-Power plant, Central Norway, Lack Behavioral Flight Responses to Wind Turbines. *Wildlife Society Bulletin* **2013**, *37*, 66–74. doi:10.1002/wsb.258.
15. Cook, A.S.C.P.; Humphreys, E.M.; Masden, E.A.; Burton, N.H.K. The Avoidance Rates of Collision Between Birds and Offshore Turbines - BTO Research Report No. 656. *Scottish Marine and Freshwater Science* **2014**, *5*.
16. Rydell, J.; Ottvall, R.; Pettersson, S.; Green, M. *Report 6791 The Effects of Wind Power on Birds and Bats*, 2017.
17. Whitfield, D.P.; Madders, M. *Deriving Collision Avoidance Rates for Red Kites *Milvus milvus**, 2006.
18. Cabrera-Cruz, S.A.; Villegas-Patraca, R. Response of Migrating Raptors to an Increasing Number of Wind Farms. *Journal of Applied Ecology* **2016**, *53*, 1667–1675. doi:10.1111/1365-2664.12673.
19. Mojica, E.K.; Watts, B.D.; Turrin, C.L. Utilization Probability Map for Migrating Bald Eagles in Northeastern North America: A Tool for Siting Wind Energy Facilities and Other Flight Hazards. *PloS one* **2016**, *11*, e0157807. doi:10.1371/journal.pone.0157807.
20. Smallwood, K.S.; Bell, D.A. Effects of Wind Turbine Curtailment on Bird and Bat Fatalities. *The Journal of Wildlife Management* **2020**, *84*, 685–696. doi:10.1002/jwmg.21844.
21. McClure, C.J.W.; Martinson, L.; Allison, T.D. Automated Monitoring for Birds in Flight: Proof of Concept with Eagles at a Wind Power Facility. *Biological Conservation* **2018**, *224*, 26–33. doi:10.1016/j.biocon.2018.04.041.
22. Marques, A.T.; Batalha, H.; Rodrigues, S.; Costa, H.; Pereira, M.J.R.; Fonseca, C.; Mascarenhas, M.; Bernardino, J. Understanding Bird Collisions at Wind Farms: An Updated Review on the Causes and Possible Mitigation Strategies. *Biological Conservation* **2014**, *179*, 40–52. doi:10.1016/j.biocon.2014.08.017.
23. Esri.; HERE.; Garmin.; FAO.; NOAA.; USGS. *World Topographic Map*, 2020. <http://www.esri.com/>.
24. Wirdheim, A.; Corell, M. *Fågelrapport*, 2015.
25. Aldén, L.; Ottvall, R.; Soares, J.P.D.S.; Klein, J.; Liljenfeldt, J. *Rapport: Samexistens Örnar och Vindkraft på Gotland*, 2017.
26. Jensen, B.B. *Efterårets Roofugletræk*. Fuglehåndbogen på Nettet, 2015.
27. IdentiFlight. *IDF Appendix*, 2019.
28. Esri. *ArcGIS Pro 2.5.0*, 2020. <http://www.esri.com/>.
29. Vattenfall AB. *Vattenfall*, 2020. <https://group.vattenfall.com/>.
30. SMHI, S.M.; Institute, H. *SMHI, Swedish Meteorological and Hydrological Institute*. Norrköping, 2020. www.smhi.se.
31. RStudio Team. *RStudio: Integrated Development Environment for R*. RStudio, PBC, Boston, MA, 2020.

-
32. Whitlock, M.C.; Schluter, D. *The Analysis of Biological Data*, 2 ed.; W. H. Freeman and Company: New York, NY, 2015.
 33. Miller, T.; Lockhart, M.; Braham, M.; Smith, B.; Katzner, T. *Flight Behavior of Golden Eagles in Wyoming: Implications for Wind Power*. American Wind Wildlife Institute: Wind Wildlife Research Meeting, 2020.
 34. Bergen, S.; Huso, M.; Braham, M.; Duerr, A.; Katzner, T.; Miller, T.; Schmuecker, S. *Improved Behavioral Classification of Flight Behavior Informs Risk Modeling of Bald Eagles at Wind Facilities in Iowa*. American Wind Wildlife Institute: Wind Wildlife Research Meeting, 2020.
 35. Kuehn, M.; Merrill, L.; Bloom, P.; Riley, E. *Temporal, Topographic, and Meteorological Correlates of Golden Eagle Flight Behavior in California's Tehachapi Wind Resource Area*. American Wind Wildlife Institute: Wind Wildlife Research Meeting, 2020.
 36. Lanzone, M.J.; Miller, T.A.; Turk, P.; Brandes, D.; Halverson, C.; Maisonneuve, C.; Tremblay, J.; Cooper, J.; O'Malley, K.; Brooks, R.P.; Katzner, T. Flight Responses by a Migratory Soaring Raptor to Changing Meteorological Conditions. *Animal Behaviour* **2012**, *8*, 710–713. doi:10.1098/rsbl.2012.0359.
 37. Wiggelinkhuizen, E.; den Boon, J. *Monitoring of Bird Collisions in Wind Farm Under Offshore-like Conditions Using WT-BIRD System*, 2010.